



P2X7 receptor inhibition by 2-amino-3-aryl-1,4-naphthoquinones

Daniela de Luna Martins^{a,*}, Adriel Alves Borges^a, Nayane A. do A. e Silva^a, Juliana Vieira Faria^{b,c}, Lucas Villas Bôas Hoelz^d, Hellen Valério Chaves Moura de Souza^d, Murilo Lamim Bello^e, Nubia Boechat^d, Vitor Francisco Ferreira^f, Robson Xavier Faria^{b,c}

^a Research Group on Catalysis and Synthesis (CSI), Universidade Federal Fluminense, Laboratório 413, Instituto de Química, Campus do Valonguinho, Centro, Niterói, RJ 24020-141, Brazil

^b Postgraduate Program in Sciences and Biotechnology, Instituto de Biologia, Universidade Federal Fluminense, Niterói, RJ, Brazil

^c Fundação Oswaldo Cruz, Instituto Oswaldo Cruz, Laboratório de Toxoplasmoses e outras protozooses, Avenida Brasil 4365, Manguinhos CEP 21045-900, Rio de Janeiro, RJ, Brazil

^d Laboratório de Síntese de Fármacos - LASFAR, Farmanguinhos - Fiocruz, Fundação Oswaldo Cruz, Rua Sizenando Nabuco, 100 - Manguinhos, Rio de Janeiro, RJ 21041-250, Brazil

^e Laboratório de Planejamento Farmacêutico e Simulação Computacional, Faculdade de Farmácia, Universidade Federal do Rio de Janeiro, Rio de Janeiro, RJ 21941-590, Brazil

^f Departamento de Tecnologia Farmacêutica, Universidade Federal Fluminense, Faculdade de Farmácia, R. Dr Mario Vianna, 523 - Santa Rosa, Niterói, RJ 24241-002, Brazil

ARTICLE INFO

Keywords:

Quinone
Purinergic receptor
Anti-inflammatory
Cation channel
Suzuki coupling

ABSTRACT

Extracellular ATP activates purinergic receptors such as P2X7, cationic channels for Ca²⁺, K⁺, and Na⁺. There is robust evidence of the involvement of these receptors in the immune response, so P2X7 receptors (P2X7R) are considered a potential therapeutic target for the development of anti-inflammatory drugs. Although there are many studies of the anti-inflammatory properties of naphthoquinones, these molecules have not yet been explored as P2X7 antagonists. In previous work, our group prepared 3-substituted (halogen or aryl) 2-hydroxy-1,4-naphthoquinones and studied their action on P2X7R. In this paper, eight 2-amino-3-aryl-1,4-naphthoquinones were evaluated to identify the inhibitory activity on P2X7R and the toxicological profile. Three analogues (AD-4CN, AD-4Me, and AD-4F) exhibited reduced toxicity for mammalian cells with CC₅₀ values higher than 500 μM. These three 3-substituted 2-amino-1,4-naphthoquinones inhibited murine P2X7R (mP2X7R) *in vitro*. However, the analogues AD-4CN and AD-4Me showed low selectivity index values. AD-4F inhibited both mP2X7R and human P2X7R (hP2X7R) with IC₅₀ values of 0.123 and 0.93 μM, respectively. Additionally, this analogue exhibited higher potency than BBG at inhibiting the ATP-induced release of IL-1β *in vitro*. Carrageenan-induced paw edema *in vivo* was reversed for AD-4F with an ID₅₀ value of 11.51 ng/kg. Although AD-4F was less potent than previous 3-substituted (halogen or aryl) 2-hydroxy-1,4-naphthoquinones such as AN-04 *in vitro*, this 3-substituted 2-amino-1,4-naphthoquinone revealed higher potency *in vivo* to reduce the edematogenic response. *In silico* analysis suggests that the binding site of the novel 2-amino-3-aryl-1,4-naphthoquinone derivatives, including all the tautomeric forms, is located in the pore area of the hP2X7R model. Based on these results, we considered AD-4F to be a satisfactory P2X7R inhibitor. AD-4F might be used as a scaffold structure to design a novel series of inhibitors with potential inhibitory activity on murine (mP2X7R) and human (hP2X7R) P2X7 receptors.

1. Introduction

Members of the P2X family (P2X1-7) are ATP-gated receptors that act as cation channels permeable to Na⁺, K⁺, and Ca²⁺. Overture of the

P2X7 receptor (P2X7R), after ATP binding, results in the passage of small cations [1,2]. Extracellular ATP can act as a danger signal, initiating inflammation by activating P2X purinergic receptors. Concerning the immune response, P2X7 is the most investigated among the

* Corresponding author.

E-mail address: dlmartins@id.uff.br (D. de Luna Martins).

URL: <https://www.danielamartinsgroup.com.br> (D. de Luna Martins).

@ (D. de Luna Martins)

<https://doi.org/10.1016/j.bioorg.2020.104278>

Received 10 March 2020; Received in revised form 10 September 2020; Accepted 11 September 2020

Available online 17 September 2020

0045-2068/ © 2020 Elsevier Inc. All rights reserved.

P2 family because it is involved with innate and adaptive immune responses. P2X7R is expressed in several cells of the immune system, such as monocytes, macrophages, lymphocytes, and other cells [3]. Several signaling pathways are connected to P2X7 activation, such as the caspase-1-containing inflammasome NLRP3, which is associated with both maturation and release of proinflammatory cytokines such as IL-1 β [4]. Therefore, P2X7 receptors are an essential target for a plethora of inflammatory pathological conditions [3,5–8].

Actually, an expressive number of commercial and synthetic substances can target P2X7R and inhibit its function [9]. Although some selective hP2X7R inhibitors exhibit promising results in clinical assays [10,11], P2X7R inhibitors have not been approved for therapeutic purposes. Consequently, there is a need to search for other inhibitors of P2X7 receptors envisaging anti-inflammatory drugs [12–14].

Naphthoquinones are privileged structures present in several compounds of biological interest [15–17]. Atovaquone, which contains the 1,4-naphthoquinone skeleton as a constituent part of its structure, is present in the atovaquone-proguanil composition employed in the treatment of malaria [18,19]. Another example of a member of the naphthoquinone group of great importance in medicinal chemistry is doxorubicin, an antineoplastic agent employed in the therapy of several types of cancer (leukemia, sarcoma, lymphoma) [20–22]. Although there are several reports of naphthoquinones with anti-inflammatory activity [23–26], this class of compounds has not been explored concerning its potential as a possible P2X7 receptor antagonist.

In our previous investigation, we prepared a series of 3-substituted 2-hydroxy-1,4-naphthoquinones through Suzuki cross-coupling reactions and studied their anti-inflammatory activity and action on human and murine P2X7 receptors. Some of these molecules have shown better results than classic P2X7 antagonists such as BBG, inhibiting IL-1 β release and the induced carrageenan paw edema [27].

In the present work, we synthesized 2-amino-3-aryl-1,4-naphthoquinones by Suzuki couplings. This new series of naphthoquinones was evaluated concerning their capacity to inhibit P2X7R receptor function *in vitro* and the acute inflammatory response *in vivo*. Additionally, we used a molecular docking approach to study the binding mode of novel naphthoquinone derivative ligands with the P2X7 receptor.

2. Results

2.1. Chemistry

Using the concept of bioisosterism, through which a prototype can be optimized in medicinal chemistry, exchanging an atom or group for another with similar chemical and biological characteristics, we used as a strategy in this work to exchange the hydroxy group for the amino group, taking as prototypes the 3-aryl-2-hydroxy-1,4-naphthoquinones from the previous work [27]. This change was also made because the amino group can be easily introduced in position 2 of the 1,4-naphthoquinone nucleus and, once present, this group increases the reactivity of the resulting naphthoquinone for iodination in position 3. This halogenation is important because organic halides are the ideal substrate for Suzuki coupling, which is our methodological strategy adopted in the synthetic sequence to obtain aryls in position 3 of the quinone nucleus.

Initially, 2-amino-1,4-naphthoquinone **2** (yield = 71%) was prepared by the reaction of 1,4-naphthoquinone **1** with hydrazoic acid, produced *in situ* by the reaction between sodium azide and acetic acid [28]. 2-Amino-1,4-naphthoquinone **2** was iodinated using a morpholine-iodine complex as the electrophile (yield = 89%). This complex was prepared from morpholine and iodine (yield = 96%), according to the procedure reported in the literature [29,30]. 2-Amino-3-iodo-1,4-naphthoquinone **3** was employed in a Suzuki cross-coupling reaction using palladium acetate as the precatalyst under microwave irradiation (Scheme 1).

As previously reported, Suzuki coupling under aqueous conditions

and using microwave irradiation proved to be an effective approach for arylation of the 3-position of 2-hydroxy-1,4-naphthoquinone [31]. Thus, in this work, we adopted these conditions as a starting point for the arylation of 2-amino-3-iodo-1,4-naphthoquinone to prepare the **AD** series of derivatives. However, some modifications were necessary to be made so that the reactions could succeed. In contrast to 3-aryl-3-hydroxy-1,4-naphthoquinones that were obtained by a fully aqueous protocol, due to solubility issues, a mixture of ethanol and water (1:1) was necessary to perform couplings with 2-amino-3-iodo-1,4-naphthoquinones to obtain 2-amino-3-aryl-1,4-naphthoquinones. Furthermore, it was necessary to employ a 5-fold higher amount of the palladium precatalyst and 2-fold higher amount of boronic acid. This procedure seems to indicate that 2-amino-3-iodo-1,4-naphthoquinone is a weaker electrophile for the Suzuki reaction than 2-hydroxy-3-iodo-1,4-naphthoquinone. A possible reason is that nitrogen is a better electron density donor than oxygen, which makes the 3-position of the 2-amino-3-iodo-1,4-naphthoquinone electronically richer than the same 3-position of the 2-hydroxy-3-iodo-1,4-naphthoquinone. The higher density at the 3-position of the 2-amino-3-iodo-1,4-naphthoquinone compared to the 3-position density of 2-hydroxy-3-iodo-1,4-naphthoquinone can be observed by the chemical shift values in the ¹³C spectrum of the compounds. 2-Amino-3-iodo-1,4-naphthoquinone exhibits a chemical shift of 82.2 ppm for carbon 3 (quinone ring), whereas 2-hydroxy-3-iodo-1,4-naphthoquinone exhibits a chemical shift of 92.7 ppm, which means that the latter is more deshielded, that is, poorer electronically.

Additionally, poor yields were achieved when an acid protocol was employed for the work-up of the reaction. Better yields were found by filtering the product and washing the solid with a basic aqueous solution, which contributed to removing some of the excesses of the boronic acid, facilitating purification of the product by flash column chromatography.

A series of 2-amino-3-aryl-1,4-naphthoquinones **AD** was obtained in moderate yields by Suzuki couplings under microwave irradiation using different arylboronic acids (Fig. 1). The decrease in yields occurred in the purification step because of the difficulty of separating the remaining boronic acids from the product by column chromatography.

2.2. Biological assays

2.2.1. Cytotoxicity studies

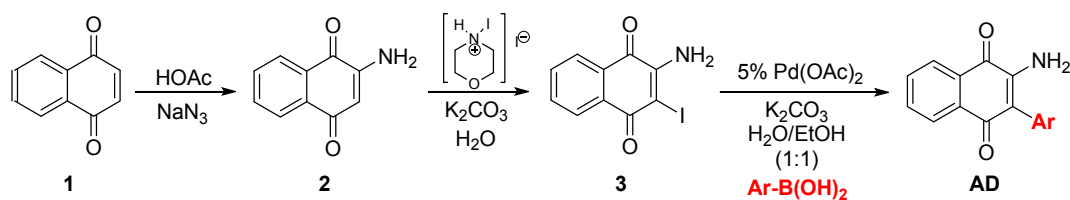
2-Amino-3-aryl-1,4-naphthoquinone derivatives affected the cytoplasmic and mitochondrial reducing enzymes from mouse peritoneal macrophages when measured for the resazurin reduction assay [32]. After continuous treatment for 24 h at a concentration of 10 μ M, all naphthoquinone analogues reduced the metabolic activity (Fig. 2). Only **AD-3F** and **AD-3T** caused a reduction higher than 25% when compared with the negative control (CN). Therefore, most of the naphthoquinones demonstrated low toxicity potential.

The amino-1,4-naphthoquinones were evaluated for their ability to inhibit P2X7R functionality in peritoneal macrophage cells. The analogues **AD-Ph**, **AD-3F**, **AD-3OMe**, and **AD-3T** did not inhibit ATP-induced dye uptake. However, **AD-4CN**, **AD-4F**, and **AD-4Me** inhibited this effect (Fig. 3).

Thus, we evaluated the cellular toxicity (for LDH release assay) of the three analogues that inhibited P2X7 receptor function (**AD-4CN**, **AD-4F**, and **AD-4Me**). The treatment at crescent concentrations for 24 h for determining the CC₅₀ value indicated low toxicity for these analogues (Fig. 4A1–A3). **AD-4CN** exhibited a CC₅₀ value of 513 μ M (Fig. 4A1). The analogues **AD-4Me** and **AD-4F** exhibited values twice as high as those of **AD-4CN**, 1000, and 1330 μ M, respectively (Fig. 4A2 and A3). These three amino-1,4-naphthoquinone analogues showed a low toxicological profile for mammalian cells.

2.2.2. 2-Amino-3-aryl-1,4-naphthoquinones inhibited P2X7 receptor function dose-dependently

AD-4CN dose-dependently reduced the ATP-induced dye uptake



Scheme 1. Synthetic sequence to 2-amino-3-aryl-1,4-naphthoquinone.

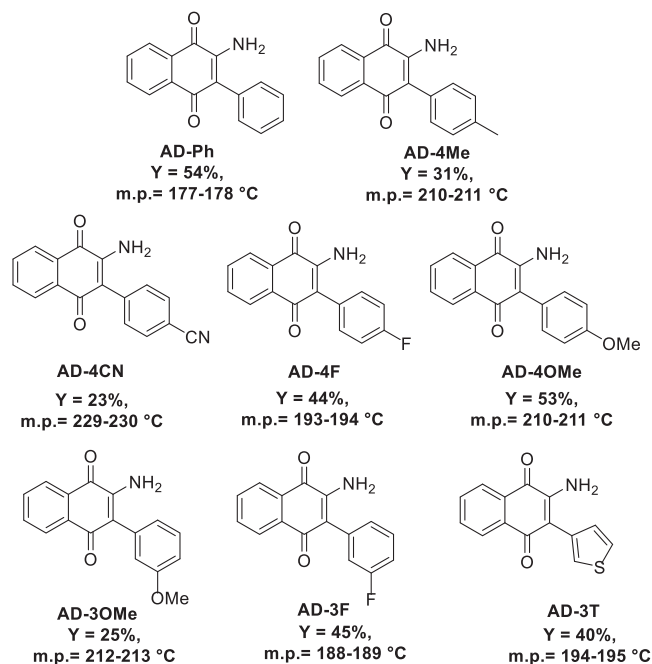


Fig. 1. 2-Amino-3-aryl-1,4-naphthoquinones obtained from Suzuki couplings.

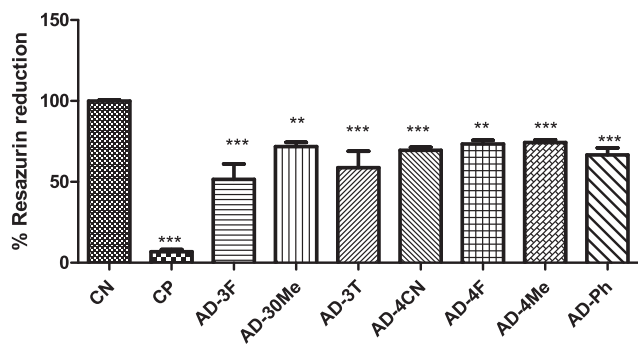


Fig. 2. 2-Amino-3-aryl-1,4-naphthoquinones toxicity on peritoneal macrophages (5.0×10^6 cells) treated for 24 h, CN- Negative control, CP- Positive control. These data are representatives of 3–4 experiments in 3 distinct days.* for $p < 0.05$, ** for a $p < 0.01$, *** for a $p < 0.001$.

assay. However, the IC_{50} value observed at $0.347 \mu\text{M}$ was near the CC_{50} value (Fig. 5B1). Thus, the selectivity index ($CC_{50}/IC_{50} = 1.47$) was low for this analogue. **AD-4Me** reduced the ATP effect with higher potency than **AD-4CN** (Fig. 5B2); in contrast, the selectivity index was also low: $CC_{50}/IC_{50} = 1.72$. The analogue **AD-4F** potently inhibited ATP-induced dye uptake when compared with the other naphthoquinone analogues ($IC_{50} = 0.123 \mu\text{M}$) (Fig. 5B3). The selectivity index calculated for **AD-4F** was 10.83. Consequently, we focused the additional assays on **AD-4F**.

BzATP-induced dye uptake in HEK 293 cells expressing the P2X7 receptor was impaired in the presence of crescent **AD-4F** concentrations

(Fig. 6). The IC_{50} value measured was $0.093 \mu\text{M}$. Therefore, this naphthoquinone was more potent at inhibiting hP2X7R.

ATP-induced IL-1 β release in the human cell lineage was inhibited by treatment with **AD-4F** added 30 min before ATP addition (Fig. 7). The IC_{50} value calculated for this inhibition was 460.9 nM .

The **AD-4F** analogue was evaluated in relation to solubility, microsomal stability, and permeability *in vitro*. This compound was stable in mouse and human microsomes (Table 1). Additionally, **AD-4F** exhibited higher permeability in Caco-2 than propranolol. This control exhibited 56% permeability, and the compound **AD-4F** exhibited 70% permeability (Table 1).

Paw edema formation after 30 min of ATP administration suffered a blunt reduction in the presence of the compound **AD-4F**. Pretreatment with compound **AD-4F** for 60 min potently inhibited edema formation (Fig. 8). The ID_{50} value measured for this naphthoquinone derivative was 11.91 ng/kg . We observed similar **AD-4F** inhibitory activity when paw edema was induced by carrageenan (Supplemental Fig. S1).

2.2.3. Molecular docking

Amino-1,4-naphthoquinone derivatives may exist in different tautomeric forms, depending on the solvent type [33,34]. Considering the physiological aqueous medium, we have taken into account the tautomerization possibility. Thus, to study the interaction of 2-amino-3-aryl-1,4-naphthoquinones to the P2X7 receptor, studies were performed for two tautomeric structures of these compounds: the amino (TAU-1) and the imino forms (TAU-2) (Scheme 2).

The molecular complexes between the three inhibitors **AD-4F**, **AD-4CN**, and **AD-4Me**, including all tautomeric forms (aminoquinone-TAU1 and iminoquinone-TAU2 forms), and the hP2X7R model (Fig. 9) were predicted using the molecular docking approach. Consequently, the ligands with the lowest energy were selected for analysis.

The molecular docking results indicated that the predicted binding site of the amino-naphthoquinone derivatives, including all the tautomeric forms, in the hP2X7R model was the same as that reported in our previous study [27]. Thus, all the compounds interact with negative values of energy within the cavity formed by Phe95(C), Phe103(C), Tyr93(C), Tyr291(C), Ser101(C), Thr94(C), Gln98(C), Leu97(A), Pro96(C), Gln98(A), and Phe102(C) (Fig. 10).

Among the inhibitors, **AD-4CN-TAU1** and **AD-4CN-TAU2** presented the highest MolDock scores, -110.42 a.u. , and -108.31 a.u. , respectively. **AD-4F-TAU1** and **AD-4F-TAU2** presented the lowest values of the MolDock score, -121.07 a.u. , and -121.27 a.u. , respectively, showing the highest affinity to the hP2X7R model. Similarly, **AD-4Me-TAU1** and **AD-4Me-TAU2** presented MolDock score values comparable to **AD-4F-TAU1** and **AD-4F-TAU2**, -121.15 a.u. , and -120.17 a.u. , respectively. In general, the MolDock score values of the 2-amino-3-aryl-1,4-naphthoquinone derivatives seem to be more favorable than those related to the 3-aryl-2-hydroxy-1,4-naphthoquinone derivatives, which were reported in our previous study [27] (Table 2).

In addition, the hydrogen bonds (H-bonds) and steric interactions were mapped using the ligand-map algorithm, generated by the MVD program. The H-bonds are represented in Fig. 11A–E. **AD-4CN-TAU1** and **AD-4CN-TAU2** interact with the hP2X7R model via H-bonds with Phe95(C) (Fig. 11A and B), presenting steric interactions with Phe95(C), Phe103(C), Ser101(C) and Gln98(A) (Table 2). **AD-4F-TAU1** forms H-bonds with Phe95 (C) and Tyr291 (C), while **AD-4F-TAU2**

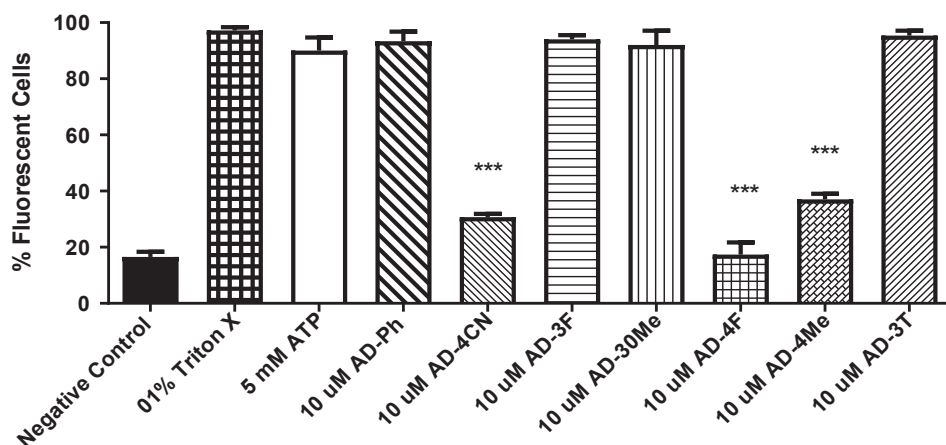


Fig. 3. 2-Amino-3-aryl-1,4-naphthoquinones reduced ATP induced dye uptake via P2X7R activation on mice peritoneal macrophages (5.0×10^6 cells). All 2-amino-3-aryl-1,4-naphthoquinones were incubated for 5 min before 5 mM ATP application for 20 min. PI dye was added in the last 5 min of ATP treatment. These data are representatives of 4–5 experiments in 3 distinct days. * for $p < 0.05$, ** for a $p < 0.01$, *** for a $p < 0.001$.

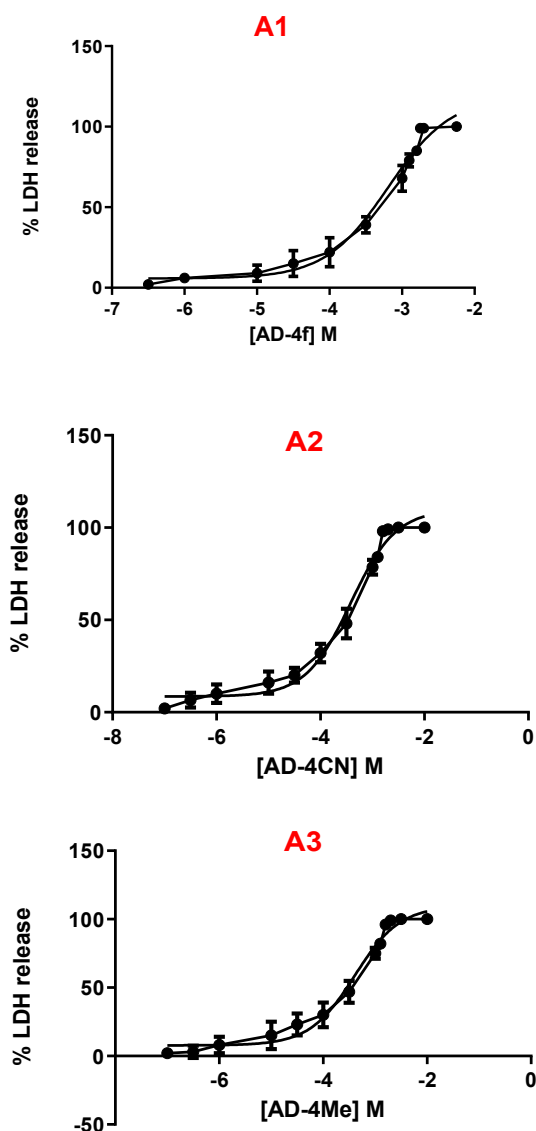


Fig. 4. 2-Amino-3-aryl-1,4-naphthoquinones induced LDH release on peritoneal macrophages (5.0×10^6 cells) treated for 24 h, CN- Negative control, CP-Positive control. These data are representatives of 3–4 experiments in 3 distinct days.

forms hydrogen bonds with Phe95 (C), Tyr291 (C), Phe103 (C), and Thr94 (C). These compounds also make steric interactions with Phe95(C), Phe103(C), Tyr93(C), and Ser101(C) (Fig. 11C and D). Nevertheless, AD-4Me-TAU1 makes H-bonds with Phe95(C) and Tyr291(C), while AD-4Me-TAU2 interacts with Phe95(C).

3. Discussion

Previously, we published 3-substituted 2-hydroxy-1,4-naphthoquinones with inhibitory activity against P2X7 receptor function. Among the tested compounds of this series, the analogues AN-03 and AN-04 showed better inhibitory activity and efficacy results *in vitro* and *in vivo* to reduce the inflammatory response [27]. As explained previously (Section 2), using the bioisosterism approach and employing 3-aryl-2-hydroxy-1,4-naphthoquinones as prototypes, the hydroxy group was replaced by the amino group, giving rise to the 2-amino-3-aryl-1,4-naphthoquinone AD series proposed in the present work.

The novel 2-amino-1,4-naphthoquinone series obtained showed higher toxicity compared to the series of 2-hydroxy-1,4-naphthoquinones [27]. All amino-1,4-naphthoquinone derivatives inhibited metabolic activity, a characteristic sometimes associated with a possible reduction in cellular viability. The toxicity of quinones may be related to their ability to induce oxidative stress in cells, which might lead to consequences such as damage to nucleic acids, destruction of proteins, lipid peroxidation and plasma membrane disruption [35].

The 2-hydroxy-1,4-naphthoquinone compounds evaluated are less toxic than the 2-amino-1,4-naphthoquinone derivatives since the CC_{50} values obtained for the hydroxy-naphthoquinones tested were all higher than 800 μ M (844–2022 μ M). These results corroborate those obtained from the resazurin tests: 2-hydroxy-1,4-naphthoquinones are less toxic than 2-amino-1,4-naphthoquinones. The presence of an amino group at the 2-position of the quinone ring instead of a hydroxy group leads to increased toxicity in the cells tested. Munday and coworkers investigated the toxicity of 2-hydroxy-1,4-naphthoquinone, 2-amino-1,4-naphthoquinone, and its derivatives against blood cells and renal cells. In this study, *in vivo*, both compounds showed toxicity to the cells and tissues surveyed [36]. Nevertheless, it was also observed that substitution at the 3-position of the naphthoquinone nucleus significantly decreased the toxicity, which was also observed in our previous work [27]. This reduction in toxicity due to substitution at the 3-position has not yet been fully elucidated. However, steric implications generated by the substituents might be among the causes, since studies have shown that, generally, small substituents do not decrease the toxicity [37]. Ring substitution of 3-aryl-2-hydroxy-1,4-naphthoquinones did not affect the toxicity of these compounds in the resazurin

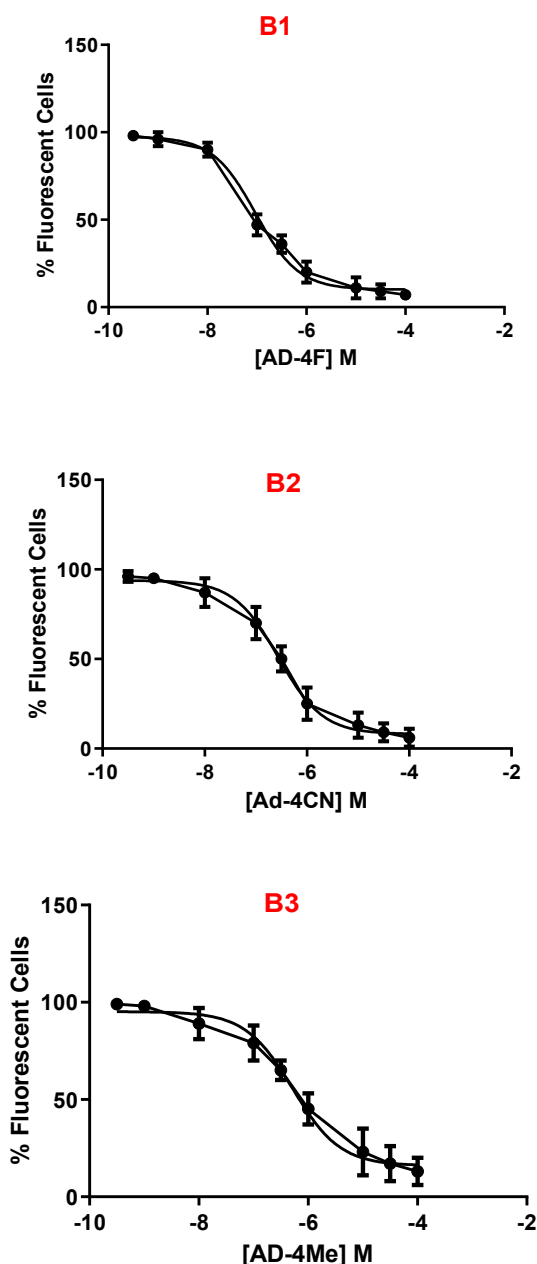


Fig. 5. AD-4F, AD-4CN, and AD-4Me dose-dependently inhibit P2X7R function in peritoneal macrophages (2.5×10^6 cells). Crescent doses of AD-4F, AD-4CN, and AD-4Me were incubated for 5 min before 5 mM ATP application for 20 min. PI dye was added in the last 5 min of ATP treatment. These data are representatives of 4–5 experiments in 3 distinct days.

test. In contrast, the presence of a ring substituent in 2-amino-1,4-naphthoquinones, regardless of the nature of the substituent, decreased the toxicity of 2-amino-1,4-naphthoquinones compared to compound AD-Ph (unsubstituted ring, Supplemental Fig. S1). Thus, for 2-amino-1,4-naphthoquinone derivatives, the steric effect may be more critical in reducing toxicity than the electronic effect.

Comparing 2-hydroxy-3-phenyl-1,4-naphthoquinone AN-04, which was the most potent inhibitor from the hydroxy-1,4-naphthoquinone series, to the most potent inhibitor AD-4F of the 2-amino-3-aryl-1,4-naphthoquinone series, it is possible to observe that an amino substituent does not improve the inhibitory effect against the P2X7 receptor. The pharmacophore 1,4-naphthoquinone core seems to have affinity to residues Phe95 and Phe103 by means of intermolecular interactions such as hydrophobic and π -stacking interactions. These

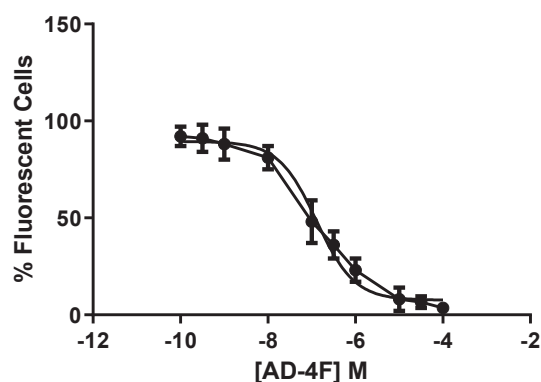


Fig. 6. AD-4F dose-dependently inhibit P2X7R function HEK 293 cells transfected with P2X7 receptor (2.5×10^6 cells). Crescent doses of AD-4F incubated for 5 min before 5 mM ATP application for 20 min. PI dye was added in the last 5 min of ATP treatment. These data are representatives of 3 experiments in 3 distinct days.

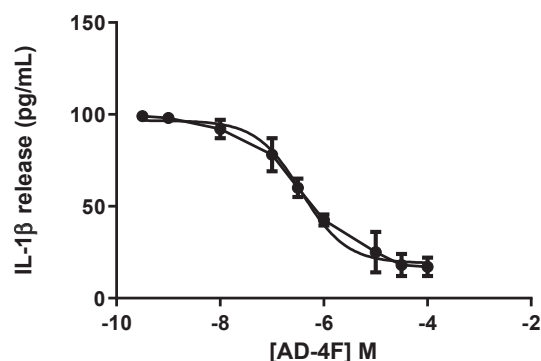


Fig. 7. ATP-induced IL-1 β release inhibition by 2-amino-3-aryl-1,4-naphthoquinones in THP-1 cells. (A) Differentiated THP-1 cells (5×10^6 cells) treated with 1 mM ATP (30 min) and LPS (4 h) in the presence of BBG, A740003, or AD-4F. The curves are representative of 3–5 independent experiments.

Table 1
Liver microsomal (LM) stability and Caco-2 data for AD-4F.

Compound	LM stability ^a mouse	LM stability ^a human	Caco-2 ^b
AD-4F	46.7	59.3	69.7 \pm 2.6

^a Stability in mice and human liver microsomes. Data reported as CL_{int} (μ L/minutes/mg protein).

^b Apparent permeability values (P_{app}) measured using low permeability and high permeability absorption compounds, vinblastine, and propranolol, respectively, as reference. Data are reported in 10⁶ cm/s. These values indicate an apical to basolateral (A - B) direction. They were tested at the same time as AD-4F. Values are means \pm standard error of 3 experiments.

residues have already been indicated in other studies as important for the binding of ligands at the allosteric site of P2X7R [38,39].

As observed for compound AN-04, the inhibitory activity of compound AD-4F is higher on hP2X7R than on mP2X7R. However, the inhibitory activity of compound AD-4F is less than the inhibitory activity of compound AN-04 on hP2X7R. The binding site indicated by docking studies is located at the pore upper area between two different subunits of the ion channel. The binding of ligands in that molecular area of P2X7R might prevent the movement of the protein, thus blocking the pore of the ion channel [38]. This binding pocket is in the same allosteric binding site area of well-known ligands, such as A740003, A804598, AZ10606120, GW791343 and JNJ47965567, which is a binding pocket distal to the ATP-binding site [39].

Although the hit compound of the series of 3-aryl-2-hydroxy-1,4-

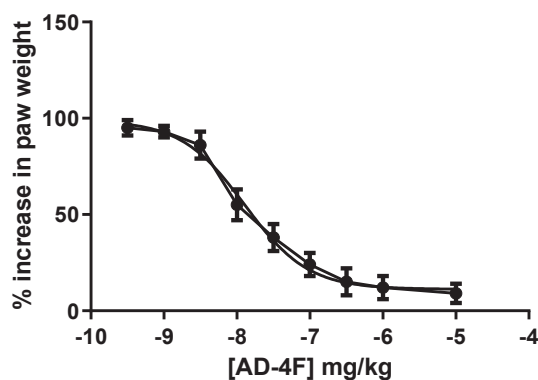
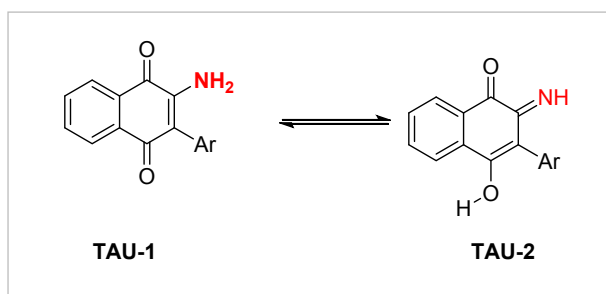


Fig. 8. AD-4F inhibits the ATP-induced paw edema. Groups containing five Swiss Webster mice that were administered with intraplantar ATP. AD-4F (0.001–1 mg/kg) (A) was administered 60 min before ATP administration, all these as control. Paw edema was measured 30 min after the ATP application. These results represent three distinct days and are expressed as mean \pm s.d.



Scheme 2. Tautomeric forms of 2-amino-3-aryl-1,4-naphthoquinones.

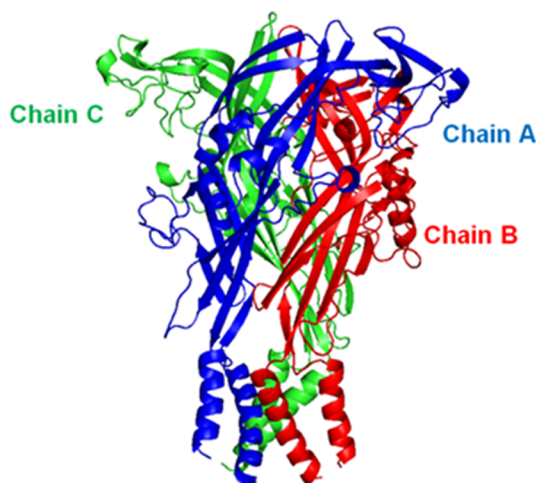


Fig. 9. Cartoon structural representation of the human P2X7 receptor (hP2X7R), showing the A (in blue), B (in red), and C (in green) chains. (For interpretation of the references to color in this figure legend, the reader is referred to the web version of this article.)

naphthoquinones showed better inhibitory activity than the hit compound of the series 2-amino-3-aryl-1,4-naphthoquinone, compound AD-4F exhibited microsomal stability 1.6 times higher (mouse and human) than compound AN-04. The compound AD-4F also presented better permeability (1.6 times higher) than the compound AN-04, which was the best P2X7R inhibitor from the hydroxy-1,4-naphthoquinone series.

The ID₅₀ value calculated for carrageenan-induced paw edema inhibition was 113 ng/kg. The hydroxy-1,4-naphthoquinone AN-04 exhibited an ID₅₀ value of 294 ng/kg for inhibiting carrageenan-induced

paw edema in a previous publication [27]. AD-4F (1 mg/kg) inhibited carrageenan-induced paw edema 2.42 times higher than sodium diclofenac (10 mg/kg) (Supplemental Fig. S1). In the previous publication, AN-04 (1 mg/kg) inhibited 0.4 times more than sodium diclofenac (10 mg/kg). This reduced AD-4F concentration to inhibit the inflammatory response compared with AN-04 may be associated with the higher permeability measured in the Caco-2 cell assay. Although AD-4F was less potent *in vitro* to inhibit P2X7 receptor function than AN-04, its higher permeability seems to compensate for this feature and cause a more potent inhibitory effect *in vivo*.

Since pH 7.4 was applied in biological assays *in vitro*, it is possible that the ionized form of compound AN-04 is predominant with deprotonated hydroxyl groups. The ionized form of the compound is less fat-soluble and better solvated in aqueous media, decreasing the molecular membrane permeability. On the other hand, the compound AD-4F probably has a higher concentration of non-ionized state molecules at pH 7.4, which might permeate more easily through the lipid bilayer membrane. As the non-ionized form of compound AD-4F might be passively transported through the lipid membranes, the acid-base equilibrium shifts to facilitate the permeation of this 2-amino-1,4-naphthoquinone derivative. The higher solvation of compound AN-04 may be responsible for hindering its passive transport across the lipid membranes compared to compound AD-4F. This possible physical-chemical property difference between the compounds seems to be in agreement with the better permeation in the Caco-2 assay presented by derivative AD-4F.

Molecular docking results showed a better score for the compound AD-4F pose than the analogue AN-04 binding pose, while the *in vitro* biological assay indicated a higher inhibitory activity of compound AN-04 than the compound AD-4F on P2X7R. Most likely, after intermolecular interactions of ligands with P2X7R, compound AN-04 stabilized the molecular complex more efficiently than compound AD-4F. It is possible to observe in the ligand binding poses that the hydrophobic interactions are important for affinity to P2X7R, and the oxygen atoms of the quinone moiety are involved in hydrogen bonds. Therefore, the substitution of hydroxyl groups by amine groups, both bioisoster substituents, in the novel 2-amino-1,4-naphthoquinone series inserted a hydrogen bond donor group that reduced the affinity of compound AD-4F to the binding site compared to compound AN-04. Nevertheless, the hit compound AD-4F showed the best performance in the *in vivo* biological evaluations.

4. Conclusions

Suzuki cross-couplings proved to be an efficient methodology for obtaining 2-amino-3-aryl-1,4-naphthoquinones, which were prepared under microwave irradiation (30 min) in moderate yields. AD-4F, AD-4Me and AD-4CN exhibited low toxicity with respect to mammalian cells (CC₅₀ > 500 μ M), and AD-4F presented the best selectivity index of the series (selectivity index CC₅₀/IC₅₀ = 10.83).

AD-4F potently inhibited mP2X7R and hP2X7R, being more active in hP2X7R inhibition (BzATP-induced dye uptake in HEK 293 cells expressing P2X7: IC₅₀ = 0.093 μ M). AD-4F was shown to be more potent than the known inhibitor BBG in ATP-induced IL-1 β release inhibition with activity on both mP2X7R (IC₅₀ = 0.544 μ M) and hP2X7R (IC₅₀ = 0.460 μ M).

The replacement of the hydroxyl group of the 2-hydroxy-1,4-naphthoquinone series used as a prototype by the amino group did not result in an improvement in the inhibitory activity on P2X7 function *in vitro*; however, the hit compound AD-4F of the novel 2-amino-1,4-naphthoquinone series showed better performance *in vivo*. That is, the presence of the amino group at position 2 of the quinone moiety resulted in improved reversion of the paw edema caused by ATP (11.51 ng/kg) and carrageenan (113 ng/kg). Derivative AD-4F also showed better performance compared to sodium diclofenac in promoting the reduction of edema. Improvement in the *in vivo* performance

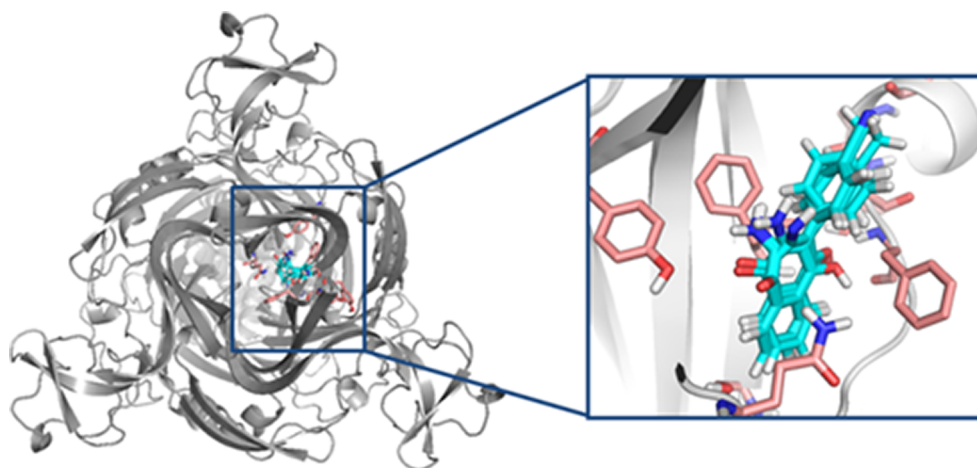


Fig. 10. Binding site of 2-amino-3-aryl-1,4-naphthoquinones derivatives in the human P2X7 receptor (hP2X7R) according to molecular docking results.

compared to the prototype compound may be related to its better microsomal stability and better permeability in the assay using Caco-2 cells.

Molecular docking studies with tautomer molecules of the most active compounds of the novel 2-amino-1,4-naphthoquinone series indicated that the binding site is located in an allosteric pocket and that hydrophobic interactions with Phe95 and Phe103 might be important for binding affinity. Therefore, the hit compound **AD-4F** seems to be promising for additional investigations.

5. Experimental section

5.1. Chemistry

Common solvents were obtained from VETEC Química. Deuterated solvents and the other reagents were purchased from Sigma Aldrich Brazil LTDA. A Fisatom 413D apparatus was employed to determine the noncorrected melting points of the products. KBr pellets were used in the infrared analysis, and spectra were recorded on a Varian FT-IR 660 spectrophotometer. A Varian VNMRs (300 or 500 MHz) instrument was utilized for recording the NMR spectra, using CDCl_3 or $\text{DMSO}-d_6$ as solvents, with chemical shifts represented in units of δ ppm. Tetramethylsilane (TMS) was used as the internal standard. Coupling constants (J , Hertz) refer to apparent multiplicities of the peak. Thin-layer chromatoplates from Silicycle Ultrapure Silica Gels (F254) were employed to monitor the progress of the reaction.

Table 2

Summary of the interactions between all tautomeric forms of each inhibitor (**AD-4CN**, **AD-4Me**, and **AD-4F**) and the human P2X7 receptor (hP2X7R) model, including the respective MolDock score values.

Inhibitors	hP2X7R		
	Residues (H-bond interaction)	Residues (steric interactions)	MolDock score (a.u.) ^a
AD-4CN-TAU1	Phe95(C)	Phe95(C), Phe103(C), Asp92(C), Ser101(C), Gln98(A)	-110.42
AD-4CN-TAU2	Phe95(C)	Phe95(C), Phe103(C), Tyr93(C), Ser101(C), Gln98(A)	-108.31
AD-4F-TAU1	Phe95(C), Tyr291(C)	Phe95(C), Phe103(C), Tyr93(C), Ser101(C)	-121.07
AD-4F-TAU2	Phe95(C), Phe103(C), Tyr291(C), Thr94(C)	Phe95(C), Phe103(C), Tyr93(C), Ser101(C)	-121.27
AD-4Me-TAU1	Phe95(C), Tyr291(C)	Phe95(C), Phe103(C), Tyr93(C), Ser101(C)	-121.15
AD-4Me-TAU2	Phe95(C), Phe103(C), Tyr291(C), Thr94(C)	Phe95(C), Phe103(C), Tyr93(C), Ser101(C), Asp92(C)	-120.17
AN02-TAU1	Tyr291(C), Ser101(C), Gln98(C)	Ser101(C), Leu97(A), Pro96(C)	-97.01
AN02-TAU2	Phe95(C), Thr94(C), Gln98(A)	Gln98(A), Ser101(C), Phe102(C), Pro96(C)	-91.29
AN03-TAU1	Gln98(C), Ser101(C), Tyr291(C)	Pro96(C), Ser101(C), Leu97(A)	-97.29
AN03-TAU2	Gln98(A), Thr94(C), Phe95(C), Phe103(C)	Thr94(C), Phe103(C), Tyr93(C)	-92.44
AN04-TAU1	Tyr291(C)	Phe95(C), Ser101(C), Pro98(A), Phe293(C)	-104.96
AN04-TAU2	Phe95(C), Phe103(C), Thr94(C)	Phe95(C), Phe103(C), Ser101(C)	-111.45

^a Arbitrary unities; ^bThe letter within the parenthesis indicates the chain of the respective residue.

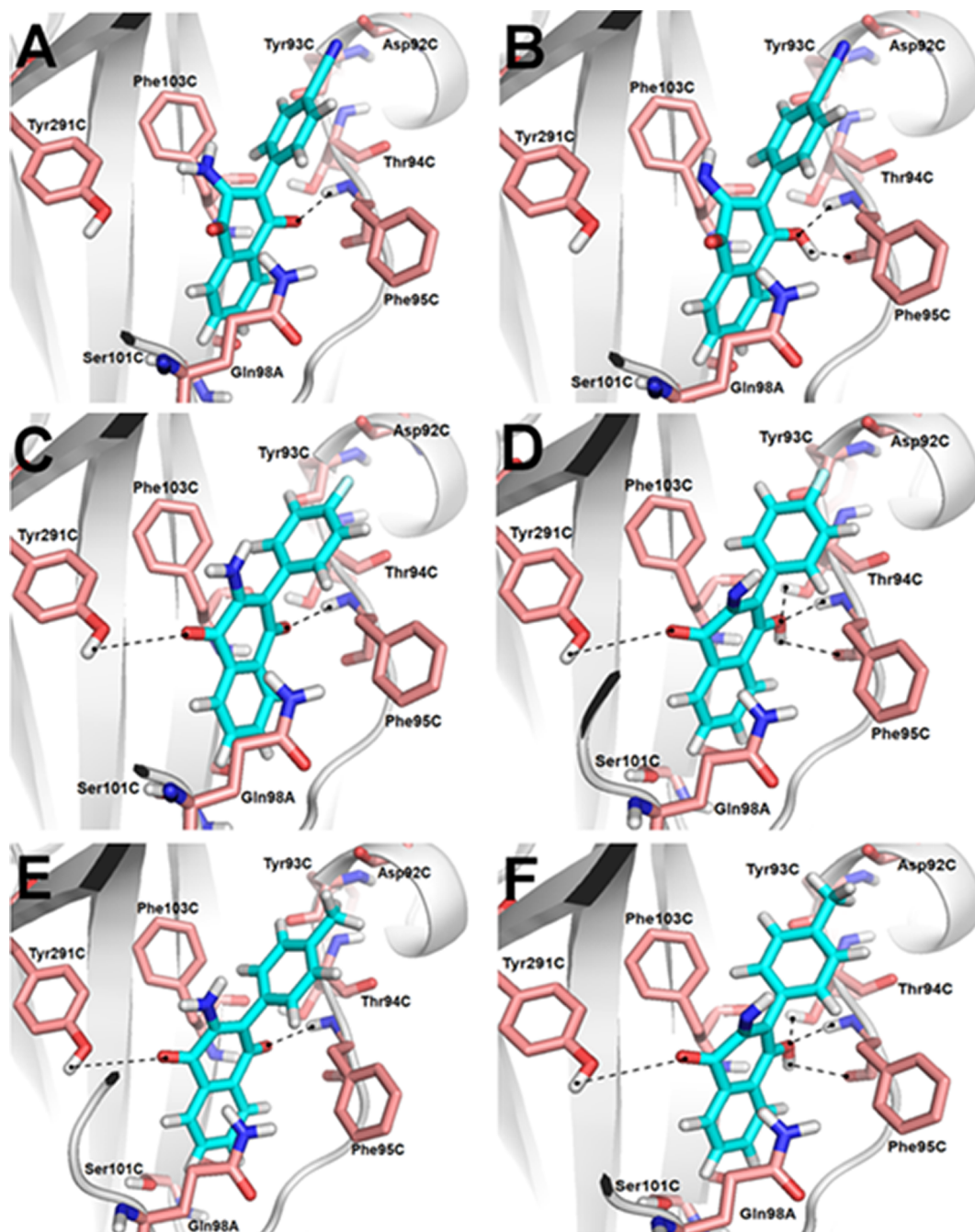


Fig. 11. Representation of the hydrogen bond interactions between the human P2X7 receptor model and the inhibitors: (A) AD-4CN-TAU1, (B) AD-4CN-TAU2, (C) AD-4F-TAU1, (D) AD-4F-TAU2, (E) AD-4Me-TAU1, and (F) AD-4Me-TAU2. The respective chain is shown within the parenthesis. Black interrupted lines represent the hydrogen bonds. The inhibitors and hP2X7R residue structures are the in stick model and colored by atom: the nitrogen atoms are shown in blue, the oxygen in red, the fluor atoms in purple, and the carbon chain in white or cyan. The hydrogen atoms were omitted for clarity, except for those present in the heteroatoms and the structure of the inhibitor. (For interpretation of the references to color in this figure legend, the reader is referred to the web version of this article.)

100 mmol). The iodine solution was dripped slowly onto the morpholine solution under vigorous agitation for 2 h. An orange solid was obtained after vacuum filtration and after washing the crude product with cold water in 96% yield. b) Iodination of 2-amino-1,4-naphthoquinone: An Erlenmeyer flask equipped with a magnetic stir bar was charged with 2-amino-1,4-naphthoquinone (30 mmol, 5.2 g), potassium carbonate (90 mmol, 12.44 g) and distilled water (300 mL). To this mixture, the morpholine-iodine complex was added in small portions every 15 min. After completion of the complex addition, the reaction mixture remained for another 30 min under stirring. Then, the reaction mixture was cooled with an ice bath and acidified with 85% H_3PO_4 . The

product was obtained after vacuum filtration, after washing with distilled water and drying, as an orange solid in 89% yield [27,29].

2-Amino-3-iodo-1,4-naphthoquinone (3) – The compound was obtained as an orange solid in 89% yield. mp 188–190 °C (lit. 201–202 °C) [26]. IR (KBr) $\nu_{\text{max}}/\text{cm}^{-1}$ 3447, 3346 (νNH_2), 1671 ($\nu \text{C}=\text{O}$), 1579 (νNH). δH (500 MHz; $\text{DMSO}-d_6$; J in Hz) 8.13–8.10 (1H, m), 7.93–7.89 (1H, m), 7.88–7.85 (1H, s) ppm. δC (125 MHz; $\text{DMSO}-d_6$) 177.3, 176.5, 152.5, 134.5, 132.5, 131.5, 129.4, 126.4, 126.3, 82.2 ppm. HRMS (ESI⁺) m/z calc. for $\text{C}_{10}\text{H}_6\text{INNaO}_2$ [$\text{M}-\text{Na}$]⁺ 322.04, found 321.9328.

5.1.3. Typical procedure for Suzuki couplings for preparing 2-amino-3-aryl-1,4-naphthoquinones

A Pyrex® 10 mL tube was charged with 2-amino-3-iodo-1,4-naphthoquinone (0.5 mmol, 150 mg), potassium carbonate (2.5 mmol, 346 mg), arylboronic acid (1.0 mmol), Pd(OAc)₂ (5% mol, 0.025 mmol) and water/ethanol 1:1 (5.0 mL). The reaction mixture was subjected to microwave irradiation (100 °C, 30 min) using a monomode microwave CEM Discover reactor. The solid product was filtered and washed with aqueous sodium hydroxide 1.0 M solution and water. The crude products were purified by flash chromatography using 75% dichloromethane/hexane.

2-Amino-3-phenyl-1,4-naphthoquinone (AD-Ph) – The compound was obtained as a red solid in 54% yield, m.p. = 177–178 °C. IR (KBr) $\nu_{\max}/\text{cm}^{-1}$ 3279 ($\nu\text{-NH}$), 1603 ($\nu\text{C=O}$), 1557 (νNH). δH (500 MHz; DMSO-*d*₆; *J* in Hz) 8.13 (1H, d, *J* = 7.5 Hz); 8.10 (1H, d, *J* = 7.0 Hz); 7.95 (1H, td, *J* = 1.0, 7.5 Hz); 7.86 (1H, td, *J* = 1.0, 7.5 Hz); 7.57 (2H, t, *J* = 7.5 Hz); 7.47 (1H, t, *J* = 7.5 Hz); 7.41–7.39 (2H, m) ppm. δC (125 MHz; DMSO-*d*₆) 181.7, 180.2, 146.1, 134.7, 130.4, 128.3, 127.3, 125.5, 114.8 ppm. HRMS (ESI⁺) *m/z* calc. for C₁₆H₁₁NNaO₂ [M – Na]⁺ 272.0684, found 272.0669.

2-Amino-3-(4-fluorophenyl)-1,4-naphthoquinone (AD-4F) – The compound was obtained as a red solid in 44% yield, m.p. = 193–194 °C. IR (KBr) $\nu_{\max}/\text{cm}^{-1}$ 3470, 3359 (νNH_2), 1674, 1674, 1601 ($\nu\text{C=O}$), 1348 (νCN). δH (500 MHz; DMSO-*d*₆; *J* in Hz) 8.00 (1H, dd, *J* = 5.0 Hz), 7.90 (1H, dd, *J* = 5.0 Hz), 7.83 (1H, td, *J* = 5.0 Hz), 7.77 (1H, td, *J* = 5.0 Hz), 7.32 (2H, m, *J* = 5.0 Hz), 7.2 (1H, m, *J* = 10.0 Hz) ppm. δC (100 MHz; DMSO-*d*₆) 181.7, 180.2, 162.6, 160.20, 146.6, 134.8, 132.7, 132.6, 132.3, 130.2, 129.6, 129.5, 125.7, 125.5, 115.4, 115.1, 113.7 ppm. HRMS (ESI⁺) *m/z* calc. for C₁₆H₁₀FNNaO₂ [M – Na]⁺ 290.0593, found 290.0578.

2-Amino-3-(3-fluorophenyl)-1,4-naphthoquinone (AD-3F) – The compound was obtained as a red solid in 45% yield, m.p. = 188–189 °C. IR (KBr) $\nu_{\max}/\text{cm}^{-1}$ 3394, 3282 (νNH_2), 1674, 1603 ($\nu\text{C=O}$), 1353 (νCN). δH (500 MHz; CDCl₃; *J* in Hz) 8.14 (1H, dd, *J* = 5.0 Hz), 8.07 (1H, dd, *J* = 5.0 Hz), 7.74 (1H, td, *J* = 5.0 Hz), 7.65 (1H, td, *J* = 5.0 Hz), 7.43 (1H, m, *J* = 10 Hz), 7.2 (1H, m, *J* = 15.0 Hz) ppm. δC (100 MHz; DMSO-*d*₆) 181.7, 179.9, 163.4, 161.0, 146.5, 135.8, 135.7, 134.9, 132.8, 132.4, 130.2, 130.2, 130.1, 126.7, 126.7, 125.8, 125.6, 117.5, 117.3, 114.2, 114.0, 113.3, 113.2 ppm. HRMS (ESI⁺) *m/z* calc. for C₁₆H₁₀FNNaO₂ [M – Na]⁺ 290.0593, found 290.0577.

2-Amino-3-(4-cyanophenyl)-1,4-naphthoquinone (AD-4CN) – The compound was obtained as an orange solid in 23% yield, m.p. = 229–230 °C. IR (KBr) $\nu_{\max}/\text{cm}^{-1}$ 3579, 3414, 3282 (νNH_2), 2233 ($\nu\text{C}\equiv\text{N}$), 1682, 1637, 1603 ($\nu\text{C=O}$). δH (500 MHz; DMSO-*d*₆; *J* in Hz) 8.15 (1H, dd, *J* = 5.0 Hz), 8.12 (1H, dd, *J* = 5.0 Hz), 7.77 (3H, M, *J* = 10.0 Hz), 7.65 (1H, td, *J* = 5.0 Hz), 7.70 (1H, td, *J* = 5.0 Hz), 7.52 (2H, d, *J* = 5.0 Hz) ppm. δC (100 MHz; DMSO-*d*₆) 181.8, 180.2, 147.0, 139.1, 135.4, 133.0, 132.9, 132.6, 132.1, 130.4, 126.2, 126.1, 119.5, 113.1, 110.1 ppm. HRMS (ESI⁺) *m/z* calc. for C₁₇H₁₀N₂NaO₂ [M – Na]⁺ 297.0640, found 297.0625.

2-Amino-3-(4-methoxyphenyl)-1,4-naphthoquinone (AD-4OMe) – Purple solid (53%), m.p. = 210–211 °C. IR (KBr) $\nu_{\max}/\text{cm}^{-1}$ 3470, 3360 (νNH_2), 1670, 1598 ($\nu\text{C=O}$), 2921 ($\nu\text{C-H}$). δH (500 MHz; DMSO-*d*₆; *J* in Hz) 8.00 (1H, dd, *J* = 5.0 Hz), 7.96 (1H, dd, *J* = 5.0 Hz), 7.84 (1H, td, *J* = 5.0 Hz), 7.72 (1H, td, *J* = 5.0 Hz), 7.21 (2H, d, *J* = 5.0 Hz), 7.19 (1H, d, *J* = 10.0 Hz), 3.84 (3H, s) ppm. δC (100 MHz; DMSO-*d*₆) 181.8, 180.1, 159.2, 146.2, 134.8, 134.6, 132.9, 132.3, 130.2, 129.4, 125.8, 125.5, 122.7, 115.8, 114.6, 113.1, 55.0 ppm. HRMS (ESI⁺) *m/z* calc. for C₁₇H₁₃NNaO₃ [M – Na]⁺ 302.0793, found 302.0774.

2-Amino-3-(3-methoxyphenyl)-1,4-naphthoquinone (AD-3OMe) – Red solid (25%), m.p. = 212–213 °C. IR (KBr) $\nu_{\max}/\text{cm}^{-1}$ 3402, 3304 (νNH_2), 1672, 1598 ($\nu\text{C=O}$), 2938 ($\nu\text{C-H}$). δH (500 MHz; CDCl₃; *J* in Hz) 8.00 (1H, dd, *J* = 5.0 Hz), 7.97 (1H, dd, *J* = 5.0 Hz), 7.84 (1H, td, *J* = 5.0 Hz), 7.73 (1H, td, *J* = 5.0 Hz), 7.21 (1H, t, *J* = 5.0 Hz), 7.19 (3H, m, *J* = 9.0 Hz), 3.85 (3H, s) ppm. δC (100 MHz; DMSO-*d*₆) 181.8, 180.4,

158.4, 146.2, 134.7, 132.9, 132.3, 131.6, 130.2, 125.7, 125.4, 125.1, 114.5, 113.9, 55.9 ppm. HRMS (ESI⁺) *m/z* calc. for C₁₇H₁₃NNaO₃ [M – Na]⁺ 302.0793, found 302.0774.

2-Amino-3-(4-methylphenyl)-1,4-naphthoquinone (AD-4Me) – Red solid (31%), m.p. = 210–211 °C. IR (KBr) $\nu_{\max}/\text{cm}^{-1}$ 3467, 3352 (νNH_2), 1670, 1598 ($\nu\text{C=O}$), 2907 ($\nu\text{C-H}$). δH (500 MHz; DMSO-*d*₆; *J* in Hz) 8.00 (1H, dd, *J* = 5.0 Hz), 7.97 (1H, dd, *J* = 5.0 Hz), 7.84 (1H, td, *J* = 5.0 Hz), 7.73 (1H, td, *J* = 5.0 Hz), 7.25 (2H, d, *J* = 5.0 Hz), 7.18 (2H, d, *J* = 5.0 Hz), 2.36 (3H, s) ppm. δC (100 MHz; DMSO-*d*₆) 181.8, 180.3, 146.2, 136.4, 134.8, 132.0, 132.2, 130.3, 130.2, 129.0, 125.8, 114.7, 21.0 ppm. HRMS (ESI⁺) *m/z* calc. for C₁₇H₁₃NNaO₂ [M – Na]⁺ 286.0844, found 286.0835.

2-Amino-3-(thiophen-3-yl)-1,4-naphthoquinone (AD-3T) – Purple solid (40%), m.p. = 210–211 °C. IR (KBr) $\nu_{\max}/\text{cm}^{-1}$ 3351 (νNH_2), 1670 ($\nu\text{C=O}$). δH (500 MHz; DMSO-*d*₆; *J* in Hz) 8.05 (2H, m), 7.94–7.937 (1H, m), 7.87 (1H, td, *J* = 15.0 Hz, 7.5 Hz), 7.82 (1H, td, *J* = 15.0 Hz), 7.56–7.53 (2H, m) ppm. δC (125 MHz; CDCl₃) 181.94, 180.71, 146.67, 135.15, 133.14, 133.10, 132.76, 130.15, 129.88, 127.01, 126.85, 125.20, 110.80 ppm. HRMS (ESI⁺) *m/z* calc. for C₁₄H₉NNaO₂S [M – Na]⁺ 278.0252, found 278.0238.

5.2. Biological assays

5.2.1. Mouse peritoneal macrophages

We used male Swiss Webster mice for the collection of macrophages from the peritoneal cavity. The protocols used were in agreement with the Ethical Principles in Animal Experimentation adopted by the Brazilian College of Animal Experimentation as well as with those approved by the FIOCRUZ Research Ethics Committee (number L039-16).

5.2.2. HEK293 cells transfected with P2X7R

Cultivation of HEK293 cells expressing P2X7R was performed supplemented with fetal bovine serum (FBS 10%), L-glutamine (2 mM) and antibiotics (streptomycin 50 µg/mL, penicillin 50 U/mL) and maintained in DMEM (Dulbecco's modified Eagle's medium) using a humidified CO₂ atmosphere (5%) at 37 °C.

5.2.3. Dye uptake assay

Before treatment with ATP, naphthoquinones and antagonists of P2X7R were preincubated for 10 min. Doses of the antagonists ranged from 1 ng to 500 µg/mL. ATP solution (5 mM) was added to mouse peritoneal macrophages (5.0 × 10⁵ cells) or HEK293 cells (5.0 × 10⁵ cells) for 25 min at 37 °C. Propidium iodide (PI) (5.0 × 10⁻² mg/mL in PBS) was added in the last five minutes of ATP treatment. After ATP treatment, we discarded the medium and added a PBS solution with 4% paraformaldehyde until measuring in an M5 Spectramax reader with excitation and emission wavelengths of 535 nm and 617 nm, respectively [27].

5.2.4. IL-1β enzyme-linked immunosorbent assay (ELISA)

THP-1 cells were primed for 4 h with LPS (25 ng/mL) prior to the experiments. At the last hour of incubation at 37 °C with LPS, AD-4F was added. At the last 30 min, ATP (5 mM) was also added. The collected treated samples were centrifuged (251.55 × g, 5 min, 4 °C), and the supernatants were stored at –70 °C. IL-1β release was measured using an ELISA Kit (ab46052-ABCAM, Cambridge).

5.2.5. pH dependent solubility of AD-4F analog

We measured the AD-4F kinetic solubility using DMSO solutions (5 µL, in triplicate) containing concentrations ranging from 1 to 250 µM. These solutions were added to 995 µL buffer (pH 2.0 - hydrochloride, 4.0–100 mM citrate buffer and 7.4–100 mM phosphate buffer) in a 96-well plate for 2 h at room temperature. Calibration standards solutions were prepared with DMSO stock solutions (5 µL) into 995 µL acetonitrile/buffer (1:1) mixture. The reaction samples were centrifuged (1118 × g, 10 min, 25 °C) and diluted 1:1 with acetonitrile [27].

5.2.6. Caco-2 cell culture and treatments

Caco-2 cells (3×10^5 cells/well) bathed with DMEM supplemented with 10% FBS were seeded on Corning®Costar®Transwell plates (Sigma-Aldrich, St. Louis, MO, USA). This culture was conserved for up to 21 days in a humidified incubator at 37 °C and 5% CO₂. **AD-4F**, vinblastine (poor permeability control), and propranolol (high permeability control) stock solutions, all at a concentration of 100 mM, were prepared in Hank's Balanced Salt Solution (HBSS) containing 25 mM HEPES at pH 7.4 with 0.5% (v/v) DMSO. Transport buffer (0.3 mL) was used to normalize the cells with the transport buffer in each well. A 24-well enhanced reposition plate with 1 mL of transport buffer (pH 7.4) substituted the feeder tray. The transport buffer in the superior wells was replaced, and 0.3 mL of the **AD-4F**, vinblastine, or propranolol solution was added. Then, the cells were substituted for incubation for 60 min. Lucifer yellow concentrations in the donor and acceptor wells were evaluated at the last incubation time. The fluorescence measurement was realized using a plate reader M5 Spectramax at excitation 485 nm and emission 530 nm.

5.2.7. In vitro stability assays in liver microsomes

AD-4F stability was assessed in male mouse and human liver microsomes [27]. Both microsomes accommodated a final protein concentration of 0.5 mg/mL (0.1 M phosphate buffer) at pH 7.4. Microsomes were preincubated with **AD-4F** (1 μM) and DMSO (0.5 μM) at 37 °C prior to NADPH (1 mM) addition. A buffer containing 0.1 M phosphate (50 μL) at pH 7.4 was used as a control for the reaction. Positive controls for mouse and human microsomes were diazepam and verapamil, respectively. Human and mouse microsomes were treated with **AD-4F** for 0, 5, 15, 30, and 45 min and the negative control (minus NADPH) for 45 min. The reactions were stopped using methanol (50 μL) at the appropriate time points. Subsequently, the samples were centrifuged (1640 × g) for 20 min at 4 °C to prevent protein precipitation.

We used the equations below for calculating *in vitro* intrinsic clearance (CL_{int mic}) for the metabolism of **AD-4F** in mouse and human liver microsomes:

$$\text{Half - life}(t_{1/2})\text{(minutes)} = 0.693/k \quad (1)$$

$$V(\mu\text{L}/\text{mg}) = \text{volume of the incubation } (\mu\text{L})/\text{protein in the incubation (mg)} \quad (2)$$

$$\text{Intrinsic clearance (CL}_{\text{int}}) (\mu\text{L}/\text{minutes}/ \text{mg protein}) = V \times 0.693/t_{1/2}$$

according to the manufacturer's instructions.

5.2.8. Paw edema

AD-4F or sodium diclofenac were administered via i.p. at 60 min before intrathecal ATP (2.5 mM/paw) or carrageenan (300 μM/paw) administration. ATP and carrageenan-induced mouse paw edema formation were measured using a plethysmometer (Insight, Brazil). This protocol obeyed the Ethical Principles in Animal Experimentation and was approved by the FIOCRUZ Research Ethics Committee (number LW-58/14).

5.2.9. Statistical analyses

The results are presented as the means ± standard deviations of the means (S.D.M.). D'Agostino and Pearson tests were used to verify whether the data followed a Gaussian distribution. In data following a Gaussian distribution, we applied an analysis of variance (ANOVA) followed by Tukey's test. Otherwise, we applied the non-parametric Kruskal-Wallis test followed by Dunn's test. PRISM® software (GraphPad, Inc., San Diego, CA, USA) was used for all statistical analyses.

5.3. In silico evaluation

5.3.1. Comparative modelling

The hP2X7R model was constructed using the approach previously described [27].

5.3.2. Ligand preparation

Chemicalize® software (ChemAxon) was employed to support the evaluation of tautomer forms and ionization states [40]. Chemical structures of the tautomers of the inhibitors were built with the aid of the program Spartan'10 v.1.0.1. (Wavefunction, Inc., Irvine, CA, USA), where the semi-empirical RM1 (Recife Model 1) method was applied for geometry optimization [41].

5.3.3. Molecular docking

Molecular docking was performed using the Molegro Virtual Docker (MVD) 6.0 program (CLC Bio, 8200, Aarhus, Denmark) [42]. The MolDock score algorithm was selected as the score function, and the partial charges were assigned according to the MVD charges scheme. The search algorithm, MolDock Optimizer, was used within a search space of 40 Å around each detected cavity in the hP2X7R model. Finally, molecular docking was performed for each tautomer using the following parameters set: runs = 100, population size = 50, max interactions = 2000, scaling factor = 0.50, and crossover rate = 0.90, followed by energy minimization. The poses with the lowest energy values were selected and analyzed using the MVD program.

Declaration of Competing Interest

The authors declare that they have no known competing financial interests or personal relationships that could have appeared to influence the work reported in this paper.

Acknowledgements

The authors are indebted to CNPq (National Council of Research of Brazil, Fellowship Process Numbers: 308755/2018-9, 455739/2014-5), CAPES and FAPERJ for funding this work and for Research fellowships (Fellowship Process Number E-26/203.246/2017, E-26/010.001861/2019; E-26/010.002125/2019). This study was financed in part by the Coordenação de Aperfeiçoamento de Pessoal de Nível Superior - Brasil (CAPES) - Finance Code 001.

Appendix A. Supplementary material

Supplementary data to this article can be found online at <https://doi.org/10.1016/j.bioorg.2020.104278>.

References

- [1] G. Burnstock, G.E. Knight, The potential of P2X7 receptors as a therapeutic target, including inflammation and tumour progression, *Purinergic Signal* 14 (2018) 1–18, <https://doi.org/10.1007/s11302-017-9593-0>.
- [2] T. Baas, Paradoxical P2X7, *SciBX5*(20) (2012). <https://doi.org/10.1038/scibx.2012.512>.
- [3] L.E.B. Savio, P.A. Mello, C.G. Silva, R. Coutinho-Silva, The P2X7 receptor in inflammatory diseases: angel or demon? *Front. Pharmacol.* 9 (2018) 52, <https://doi.org/10.3389/fphar.2018.00052>.
- [4] R. Barlett, L. Stokes, R. Sluyter, The P2X7 receptor channel: recent developments and the use of P2X7 antagonists in models of disease, *Pharmacol. Rev.* 66 (2014) 638–675, <https://doi.org/10.1124/pr.113.008003>.
- [5] L.A. Alves, R.J.S. Bezerra, R.X. Faria, L.G.B. Ferreira, V.S. Frutuoso, Physiological roles and potential therapeutic applications of the P2X7 receptor in inflammation and pain, *Molecules* 18 (2013) 10953–10972, <https://doi.org/10.3390/molecules180910953>.
- [6] T. Gicquel, B. Le Dare, E. Boichot, V. Lagente, Purinergic receptors: new targets for the treatment of gout and fibrosis, *Fundam. Clin. Pharmacol.* 31 (2017) 136–146, <https://doi.org/10.1111/fcp.12256>.
- [7] J.C. Rech, A. Bhattacharya, M.A. Letavic, B.M. Savall, The evolution of P2X7 antagonists with a focus on CNS indications, *Bioorg. Med. Chem. Lett.* 26 (2016)

- 3838–3845, <https://doi.org/10.1016/j.bmcl.2016.06.048>.
- [8] E. Beamer, W. Fischer, T. Engel, The ATP-gated P2X7 receptor as a target for the treatment of drug-resistant epilepsy, *Front. Neurosci.* 11 (2017) 21, <https://doi.org/10.3389/fnins.2017.00021>.
- [9] C.E. Müller, Y. Bagi, V. Namasivayam, Agonists and antagonists for purinergic receptors, *Methods Mol. Biol.* 2041 (2020) 45–64, https://doi.org/10.1007/978-1-4939-9717-6_3.
- [10] M. Timmers, P. Ravenstijn, L. Xi, G. Triana-Baltzer, M. Furey, S. Van Hemelryck, J. Biewenga, M. Ceusters, A. Bhattacharya, M. van den Boer, L. Van Nueten, P. de Boer, Clinical pharmacokinetics, pharmacodynamics, safety, and tolerability of JNJ-54175446, a brain permeable P2X7 antagonist, in a randomised single-ascending dose study in healthy participants, *Psychopharmacol.* 32 (2018) 1341–1350 <https://journals.sagepub.com/doi/10.1177/0269881118800067>.
- [11] L.K. Kan, S. Seneviratne, K.J. Drummond, D.A. Williams, T.J. O'Brien, M. Monif, P2X7 receptor antagonism inhibits tumour growth in human high-grade gliomas, *Purinergic Signal* (2020), <https://doi.org/10.1007/s11302-020-09705-2>.
- [12] N. Mehta, M. Kaur, M. Singh, S. Chand, B. Vyas, P. Silakari, M.S. Bahia, O. Silakari, Purinergic receptor P2X7: a novel target for anti-inflammatory therapy, *Bioorg. Med. Chem.* 22 (2014) 54–88, <https://doi.org/10.1016/j.bmc.2013.10.054>.
- [13] L.H. Jiang, S. Roger, Targeting the P2X7 receptor in microglial cells to prevent brain inflammation, *Neural Regen. Res.* 15 (2020) 1245–1246, <https://doi.org/10.4103/1673-5374.272575>.
- [14] D.T. Gonzaga, L.B.G. Ferreira, T.E.M.M. Costa, N.L. von Ranke, P.A.F. Pacheco, A.P.S. Simões, J.C. Arruda, L.P. Dantas, H.R. Freitas, R.A.M. Reis, C. Penedo, M.L. Bello, H.C. Castro, C.R. Rodrigues, V.F. Ferreira, R.X. Faria, F.C. da Silva, 1-Aryl-1H- and 2-aryl-2H-1,2,3-triazole derivatives blockade P2X7 receptor *in vitro* and inflammatory response *in vivo*, *Eur. J. Med. Chem.* 239 (2018) 698–717, <https://doi.org/10.1016/j.ejmech.2017.08.034>.
- [15] V.F. Ferreira, F.C. da Silva, Strategies for the synthesis of bioactive pyran naphthoquinones, *Org. Biomol. Chem.* 8 (2010) 4793–4802, <https://doi.org/10.1039/C0OB00277A>.
- [16] A.K. Jordão, M.D. Vargas, A.C. Pinto, F.C. da Silva, V.F. Ferreira, Lawsone in organic synthesis, *RSC Adv.* 5 (2015) 67909–67943, <https://doi.org/10.1039/C5RA12785H>.
- [17] G.A.M. Jardim, W.X.C. Oliveira, R.P. de Freitas, R.F.S. Menna-Barreto, T.L. Silva, M.O.F. Goulart, E.N.S. Júnior, Direct sequential C-H iodination/organoyl-thiolation for the benzenoid A-ring modification of quinonoid deactivated systems: a new protocol for potent trypanocidal quinones, *Org. Biomol. Chem.* 16 (2018) 1686–1691, <https://doi.org/10.1039/C8OB00196K>.
- [18] S.Y. Dike, D. Singh, B.N. Thankachen, B. Sharma, P.K. Mathur, S. Kor, A. Kumar, A single-pot synthesis of atovaquone: an antiparasitic drug of choice, *Org. Process Res. Dev.* 18 (2014) 618–625, <https://doi.org/10.1021/op500032w>.
- [19] a) K. McKeage, L. Scott, Atovaquone/proguanil: a review of its use for the prophylaxis of *Plasmodium falciparum* malaria, *Drugs* 63 (2003) 597–623, <https://doi.org/10.2165/00003495-200363060-00006>;
b) L.G. Haile, J.F. Faherty, Atovaquone: a review, *Ann. Pharmacother.* 27 (1993) 1488–1494 <https://doi.org/10.1177/106002809302701215>.
- [20] O. Tacar, P. Sriamornsak, C.R. Dass, Doxorubicin: an update on anticancer molecular action, toxicity and novel drug delivery systems, *J. Pharm. Pharmacol.* 65 (2013) 157–170, <https://doi.org/10.1111/j.2042-7158.2012.01567.x>.
- [21] A. Shafei, W. El-Bakly, A. Sobny, O. Wagdy, A. Reda, O. Aboelenin, A. Marzouk, K. El Habak, R. Mostafa, M.A. Ali, M. Ellithy, A review on the efficacy and toxicity of different doxorubicin nanoparticles for targeted therapy in metastatic breast cancer, *Biomed. Pharmacother.* 95 (2017) 1209–1218, <https://doi.org/10.1016/j.biopha.2017.09.059>.
- [22] J. Lao, J. Madani, T. Puértolas, M. Alvarez, A. Hernández, R. Pazo-Cid, A. Artal, A.A. Torres, Liposomal doxorubicin in the treatment of breast cancer patients: a review, *J. Drug Deliv.* 2013 (2013) 456409, <https://doi.org/10.1155/2013/456409>.
- [23] P.A.F. Pacheco, R.M.S. Galvão, A.F.M. Faria, N.L. Von Ranke, M.S. Rangel, T.M. Ribeiro, C.R. Rodrigues, V.F. Ferreira, D.R. da Rocha, R.X. Faria, 8-Hydroxy-2-(1H-1,2,3-triazol-1-yl)-1,4-naphthoquinone derivatives inhibited P2X7 Receptor-induced dye uptake into murine Macrophages, *Bioorg. Med. Chem.* 27 (2019) 1449–1455, <https://doi.org/10.1016/j.bmc.2018.11.036>.
- [24] S.A. Pai, R.P. Munshi, F.H. Panchal, I.S. Gaur, S.N. Gursahani, A.R. Juvekar, Plumbagin reduces obesity and nonalcoholic fatty liver disease induced by fructose in rats through regulation of lipid metabolism, inflammation and oxidative stress, *Biomed. Pharmacother.* 111 (2019) 686–694, <https://doi.org/10.1016/j.biopha.2018.12.139>.
- [25] K. Kobayashi, K.S. Nishiumi, M. Nishida, M. Hirai, T. Azuma, H. Yoshida, Y. Mizushima, M. Yoshida, Effects of quinone derivatives, such as 1,4-naphthoquinone, on DNA polymerase inhibition and anti-inflammatory action, *Med. Chem.* 7 (2011) 37–44, <https://doi.org/10.2174/157340611794072742>.
- [26] P. Luo, Y.F. Wong, L. Ge, Z.F. Zhang, Y. Liu, H. Zhou, Anti-inflammatory and analgesic effect of plumbagin through inhibition of nuclear factor- κ B activation, *J. Pharmacol. Exp. Ther.* 335 (2010) 735–742, <https://doi.org/10.1124/jpet.110.170852>.
- [27] R.X. Faria, F.H. Oliveira, J.B. Sales, A.S. Oliveira, N.I. Von Ranke, M.L. Bello, C.R. Rodrigues, H.C. Castro, A.R. Louvis, D.L. Martins, V.F. Ferreira, 1,4-Naphthoquinones potently inhibiting P2X7 receptor activity, *Eur. J. Med. Chem.* 143 (2018) 1361–1372, <https://doi.org/10.1016/j.ejmech.2017.10.033>.
- [28] J.L. Hartwell, L.F. Fieser, The reaction of hydrazoic acid with the naphthoquinones, *J. Am. Chem. Soc.* 57 (1935) 1482–1484, <https://doi.org/10.1021/ja01311a030>.
- [29] A.L. Perez, G. Lamoureux, A. Herrera, Synthesis of iodinated naphthoquinones using morpholine-iodine complex, *Synth. Commun.* 34 (2004) 3389–3397, <https://doi.org/10.1081/SCC-200030621>.
- [30] L.C.R.M. da Frota, R.C.P. Canavez, S.L.S. Gomes, P.R.R. Costa, A.J.M. da Silva, Iodination of phenols in water using easy to handle amine-iodine complexes, *J. Braz. Soc. Soc.* 20 (2009) 1916–1920, <https://doi.org/10.1590/S0103-50532009001000021>.
- [31] A.R. Louvis, N.A.A. e Silva, F.S. Semaan, F.C. da Silva, G. Saramago, L.C.S.V. de Souza, B.L.A. Ferreira, H.C. Castro, J.P. Salles, A.L.A. Souza, R.X. Faria, V.F. Ferreira, D.L. Martins, Synthesis, characterization and biological activities of 3-aryl-1,4-naphthoquinones – greenpalladium-catalysed Suzuki cross coupling, *Chem.* 40 (2016) 7643–7656, <https://doi.org/10.1039/C6NJ00872K>.
- [32] R. Csepregi, B. Lemli, S. Kunsági-Máté, L. Szente, T. Kőszegi, B. Némethi, M. Poór, Complex formation of resorufin and resazurin with β -cyclodextrins: Can cyclodextrins interfere with a resazurin cell viability assay? *Molecules* 23 (2018) 382–398, <https://doi.org/10.3390/molecules23020382>.
- [33] F. Louis, M. Fieser, The tautomerism of the aminonaphthoquinones, *J. Am. Chem. Soc.* 56 (1934) 1565–1578, <https://doi.org/10.1021/ja01322a034>.
- [34] S. Bhand, R. Patil, Y. Shinde, D.N. Lande, S.S. Rao, L. Kathawate, S.P. Gejji, T. Weyhermüller, S. Salunke-Gawali, Tautomerism in *O*-hydroxyanilino-1,4-naphthoquinone derivatives: structure, NMR, HPLC and density functional theoretic investigations, *J. Mol. Struct.* 1123 (2016) 245–260, <https://doi.org/10.1016/j.molstruc.2016.06.026>.
- [35] D.M. Hernández, M.A.B.F. De Moura, D.P. Valencia, F.J. González, I. González, F.C. de Abreu, E.N.S. Júnior, V.F. Ferreira, A.V. Pinto, M.O.F. Goulart, C. Frontana, Inner reorganization during the radical–biradical transition in a nor- β -lapachone derivative possessing two redox centers, *Org. Biomol. Chem.* 6 (2008) 3414–3420, <https://doi.org/10.1039/B806271D>.
- [36] R. Munday, B.L. Smith, C.M. Munday, Structure-activity relationships in the haemolytic activity and nephrotoxicity of derivatives of 1,2- and 1,4-naphthoquinone, *J. Appl. Toxicol.* 27 (2007) 262–269, <https://doi.org/10.1002/jat.1206>.
- [37] R. Munday, B.L. Smith, C.M. Munday, Effect of butylated hydroxyanisole on the toxicity of 2-hydroxy-1,4-naphthoquinone to rats, *Chem. Biol. Interact.* 117 (1999) 241–256, [https://doi.org/10.1016/S0009-2797\(98\)00108-2](https://doi.org/10.1016/S0009-2797(98)00108-2).
- [38] E.G. dos Santos, R.X. Faria, C.R. Rodrigues, M.L. Bello, Molecular dynamic simulations of full-length human purinergic receptor subtype P2X7 bonded to potent inhibitors, *Eur. J. Pharm. Sci.* 152 (2020) 1–12, <https://doi.org/10.1016/j.ejps.2020.105454>.
- [39] A. Karasawa, T. Kawate, Structural basis for subtype-specific inhibition of the P2X7 receptor, *eLife* 5 (2016) 1–17, <https://doi.org/10.7554/eLife.22153>.
- [40] M. Swain, Chemicalize.org, *J. Chem. Inf. Model.* 52 (2012) 613–615, <https://doi.org/10.1021/ci300046g>.
- [41] G.B. Rocha, R.O. Freire, A.M. Simas, J.J.P. Stewart, RM1: A reparameterization of AM1 for H, C, N, O, P, S, F, Cl, Br, I, *J. Comp. Chem.* 27 (2006) 1101–1111, <https://doi.org/10.1002/jcc.20425>.
- [42] R. Thomsen, M.H. Christensen, MolDock: a new technique for high-accuracy molecular docking, *J. Med. Chem.* 49 (2006) 3315–3321, <https://doi.org/10.1021/jm051197e>.